American Mineralogist, Volume 92, pages 1242–1245, 2007

LETTER

Crystal-structure refinement of Na-bearing clinopyroxenes from mantle-derived eclogite xenoliths

FABRIZIO NESTOLA,* MICAELA LONGO, CATHERINE MCCAMMON, AND TIZIANA BOFFA BALLARAN

Bayerisches Geoinstitut, Universität Bayreuth, D-95440 Bayreuth, Germany

ABSTRACT

Nine omphacitic clinopyroxenes with a jadeitic content between 25% and 57% from the Udachnaya and Zagadochnaya diamond-bearing kimberlites were investigated using single-crystal X-ray diffraction, electron microprobe analysis, and Mössbauer and infrared spectroscopy. Crystal-structure refinements, incorporating constraints from chemical analyses and Mössbauer data, show a significant concentration of vacancies at the M2 site in three of the samples. The cell volumes of the non-stoichiometric samples plot below the linear trend defined by stoichiometric diopside-jadeite compositions, where the deviation from the linear trend is positively correlated with the concentration of vacancies. Charge-balance appears to be achieved primarily through substitution of Al^{3+} for Mg^{2+} on the M1 site, which causes a contraction of the M1 site volume compared to stoichiometric clinopyroxenes with the same composition. Vacancies are not associated with OH^- incorporation, as the sample with the highest concentration of vacancies contains only 89 ppm (wt) H_2O. Significant hydrogen loss through iron oxidation during ascent is ruled out based on the low Fe^{3+} concentrations. H content in omphacite samples from kimberlites could provide a sensitive tool for determining f_{H_2O} during diamond formation.

Keywords: Crystal structure, omphacite, non-stoichiometry, water

INTRODUCTION

Omphacitic clinopyroxene and pyropic garnet represent the main constituents of mantle-derived eclogite; therefore, their structure and chemistry provides clues to the conditions under which the eclogite formed. Clinopyroxene from mantle-derived eclogite xenoliths shows deviations from stoichiometry based on their cation sums, suggesting the presence of vacancies at M sites (e.g., Sobolev et al. 1968; Smyth 1980; McCormick 1986; Oberti and Caporuscio 1991). The presence of cation vacancies in clinopyroxenes has been linked to OH^- substitution in the crystal structure (Smyth et al. 1991; Katayama and Nakashima 2003; Koch-Müller et al. 2004). However, studies of hydrogen concentration in clinopyroxenes from diamond-bearing eclogite xenoliths have shown them to be dry, despite their apparent non-stoichiometry (Koch-Müller et al. 2004). To examine more accurately the relation between hydrogen content and structural vacancies in omphacitic clinopyroxene, we made a detailed study of nine well-characterized clinopyroxenes from mantle-derived eclogite xenoliths using single-crystal X-ray diffraction, electron microprobe analysis, and Mössbauer and infrared spectroscopy.

EXPERIMENTAL METHODS

The sample suite comprised nine handpicked separates of clinopyroxene extracted from eclogite xenoliths from the Zagadochnaya kimberlite (sample 90-394) and the Udachnaya kimberlite (all other samples), both in the Yakutia craton (Russia). The composition of major elements was determined using a wavelength-dispersive JEOL electron microprobe (JXA-8200) operating at 15 keV and 15 nA. Analyses were averaged over a minimum of 20 points collected for each sample (Table 1). Crystallization temperatures determined from Fe/Mg exchange between garnet and clinopyroxene (Ellis and Green 1979) ranged from 900 to 1300 °C assuming a pressure of 5 GPa.

Mössbauer spectra were recorded at room temperature and 80 K using a conventional transmission spectrometer with a nominal 1.85 GBq ^{57}Co(Rh) source with velocity calibration relative to α-Fe. Approximately 5 mg of handpicked grains from each sample were used, giving absorber thicknesses of 1–2 mg Fe/cm^2. Mössbauer spectra from different temperatures for each sample were simultaneously fitted incorporating center shift variations due to the second-order Doppler shift and area fraction variations due to differences in recoil-free fraction. This procedure enabled the determination of robust Fe^{3+} concentrations (Table 1).

Hydrogen concentration was measured using Fourier-transform infrared (FTIR) spectroscopy. Water contents were derived from integral absorbances measured by taking polarized spectra with the electrical field vector parallel to the three axes of the indicatrix. Only one band was seen at 3470 cm^{-1} with maximum absorption parallel to γ, as is usual for omphacites (Skogby 2006). The total water content was obtained using the integral extinction coefficient by Bell et al. (1995).

One single crystal of each clinopyroxene sample was selected (maximum crystal size between 200 and 400 μm) for complete intensity data collection based on its sharp optical extinction and absence of twinning. Optical examination revealed that crystals were defect- and inclusion-free. Intensity data were collected at ambient conditions using a Kappa geometry Xcalibur diffractometer with graphite monochromated Mo$K\alpha$ radiation. The intensity data were measured in the $5 \leq 2\theta \leq 80°$ range using the ω-scan mode with a continuous-integrative step scan (0.05°/s, 60 scan steps, scan width 1.2°). The sample-detector distance was 135 mm. A careful analysis of the diffraction profiles excluded the presence of multiple chains (e.g., amphibole lamellae) as expected for unaltered and defect-free samples. The program Win-IntegrStp (version 3.3, Angel 2003) was used to integrate the step-scan data applying the Lorentz-polarization correction. The integrated data were then corrected for absorption using the program ABSORB V6.0 (Angel 2004).

Weighted structural refinements based on F_o^2 were performed using the SHELX-97 package (Sheldrick 1997) in the *C*2/*c* space group starting from the coordinates of McCormick (1986). The atomic scattering factors were taken from the *International Tables for X-Ray Crystallography* (Wilson 1995). Neutral vs. ionized scattered curves were refined for the oxygen (O and O^{-2}) and silicon (Si

* Present address: Dipartimento di Geoscienze, Università Padova, I-10137 Padova, Italy. E-mail: fabrizio.nestola@unipd.it

0003-004X/07/0007–1242$05.00/DOI: 10.2138/am.2007.2654

TABLE 1. Chemical composition of clinopyroxenes determined by electron microprobe and Mössbauer and FTIR spectroscopy

Samples wt%	U947	Ud2290	Ud160	Ud146	90-394	Ud94	Ud31	90-390	Ud685
SiO_2	56.50(1.04)	56.41(50)	55.76(55)	55.43(58)	54.55(35)	55.57(38)	54.90(49)	54.25(42)	55.65(41)
TiO_2	0.23(3)	0.21(3)	0.43(3)	0.62(2)	0.06(3)	0.57(3)	0.49(3)	0.41(5)	0.16(4)
Al_2O_3	16.34(30)	15.71(33)	10.68(31)	7.88(18)	11.99(30)	9.45(25)	5.17(13)	6.12(15)	6.17(27)
Cr_2O_3	0.03(3)	0.04(2)	0.08(3)	0.07(2)	0.15(2)	0.07(2)	0.08(2)	0.04(2)	0.10(3)
FeO*	1.92(4)	2.64(5)	5.16(8)	6.08(7)	1.72(4)	5.15(7)	7.79(8)	7.86(9)	3.03(8)
MnO	0.03(4)	0.02(2)	0.04(3)	0.09(5)	0.02(2)	0.07(4)	0.09(4)	0.09(3)	0.05(5)
MgO	5.88(5)	6.02(7)	9.32(7)	12.21(8)	9.72(9)	10.69(14)	14.40(9)	10.29(9)	13.09(9)
CaO	10.03(14)	9.93(17)	11.09(11)	11.57(21)	16.51(22)	11.75(17)	12.16(26)	16.34(17)	18.15(13)
Na_2O	7.91(9)	8.19(9)	7.05(9)	5.47(7)	4.71(8)	6.36(13)	4.28(11)	4.16(8)	3.58(4)
K_2O	0.20(2)	0.03(1)	0.07(1)	0.13(1)	0.04(1)	0.05(1)	0.07(1)	0.01(1)	0.19(14)
H_2O†	0.0089	n.a.	n.a.	n.a.	n.a.	n.a.	n.a.	n.a.	n.a.
Total	99.07	99.19	99.67	99.54	99.45	99.73	99.42	99.56	100.16
Cation per six O atoms determined by microprobe analyses									
Si	1.980(36)	1.982(18)	1.990(20)	1.992(21)	1.939(12)	1.986(14)	1.996(18)	1.991(15)	1.991(15)
Ti	0.006(1)	0.006(1)	0.012(1)	0.017(1)	0.002(1)	0.015(1)	0.013(1)	0.011(1)	0.004(1)
Al	0.675(13)	0.651(14)	0.449(13)	0.334(8)	0.502(12)	0.398(11)	0.221(5)	0.265(7)	0.260(11)
Cr	0.001(1)	0.001(1)	0.002(1)	0.002(1)	0.004(1)	0.002(1)	0.002(1)	0.001(1)	0.003(1)
Fe^{2+}‡	0.048(2)	0.056(2)	0.116(5)	0.146(4)	0.043(2)	0.112(4)	0.174(5)	0.213(5)	0.080(3)
Fe^{3+}‡	0.009(1)	0.021(2)	0.038(4)	0.037(4)	0.008(1)	0.042(3)	0.063(5)	0.028(4)	0.010(1)
Mn	0.001(1)	0.000(1)	0.001(1)	0.003(2)	0.001(1)	0.002(1)	0.003(1)	0.003(1)	0.001(1)
Mg	0.307(3)	0.315(4)	0.496(4)	0.654(4)	0.515(5)	0.570(7)	0.780(5)	0.563(5)	0.698(5)
Ca	0.376(5)	0.374(7)	0.424(4)	0.445(8)	0.629(8)	0.450(7)	0.473(10)	0.642(7)	0.696(5)
Na	0.537(6)	0.558(6)	0.488(6)	0.381(5)	0.325(5)	0.441(9)	0.302(8)	0.296(5)	0.248(3)
K	0.009(1)	0.001(1)	0.003(1)	0.006(1)	0.002(1)	0.002(1)	0.003(1)	0.000(1)	0.009(6)
Total	3.949(40)	3.966(24)	4.018(25)	4.016(25)	3.969(21)	4.020(22)	4.031(23)	4.013(20)	4.001(21)

Note: Standard deviations are given in parentheses; n.a. = not analyzed.
* Fe is calculated as FeO.
† H_2O determined by FTIR.
‡ Fe^{2+}/Fe^{3+} ratios determined by Mössbauer spectroscopy.

and Si^{2+} atoms). Fully ionized scattering factors were used for Al^{3+}, Ti^{4+}, Cr^{3+}, Mg^{2+}, Fe^{2+}, Fe^{3+}, Mn^{2+}, Ca^{2+}, Na^{+}, and K^{+}. Anisotropic thermal parameters were obtained for all atoms. A residual electron-density maximum, located at 0.6–0.7 Å from the M2 site, was observed in the difference-Fourier map for all crystals. The same feature has been observed in previous studies (Rossi et al. 1987; Oberti and Caporuscio 1991; Boffa Ballaran et al. 1998) and it has been attributed to the combined presence of Mg and Fe^{2+} at the M2 site, giving rise to a M2' split position. Therefore, a further set of refinements were performed using Mg^{2+} and Fe^{2+} scattering factors for the isotropic M2' site.

To obtain accurate site populations, constraints were introduced into the refinements following a procedure similar to that used by Domeneghetti et al. (2005): (1) chemical constraints were taken from the electron microprobe analysis results; (2) Fe^{3+} was constrained to the value obtained from Mössbauer spectroscopy; (3) the tetrahedral T and the octahedral M1 sites were considered fully occupied (Smyth 1980; McCormick 1986; Oberti and Caporuscio 1991), whereas the occupancy of the M2 + M2' sites was allowed to be less than 1 to account for deviations from stoichiometry; (4) Al^{3+} was distributed between the tetrahedral T and the octahedral M1 sites; (5) Fe^{3+}, Cr^{3+}, and Ti^{4+} were considered fully ordered at the M1 site; (6) Mg^{2+} and Fe^{2+} were allowed to fractionate between the M1 and the M2' sites; (7) Mn^{2+} was considered fully ordered at the M2 site (Stimpfl 2005); (8) Ca^{2+}, Na^{+} and K^{+} were assumed to occupy the M2 site; (9) charge balance was constrained by the equation: $X_{Fe^{3+}} + X_{Al^{6+}} + X_{Cr} + 2X_{Ti} = X_{Al^{4+}} + X_{Na} + X_{K}$.

RESULTS AND DISCUSSION

Results of the refinements and site populations are reported in Table 2, and atomic coordinates and displacement parameters, octahedral and tetrahedral bond distances, and volumes are reported in Tables 3[1] and 4[1]. All of the clinopyroxenes analyzed in this study only show reflections within the *C*2/*c* space group, which rules out suggestions of incipient cation ordering and reduction of the symmetry to *P*2/*n*. All estimated equilibration temperatures are above the critical temperature of the *P*2/*n*-*C*2/*c* transition (~850 °C) inferred by Carpenter (1981).

All the investigated clinopyroxenes have a low amount of Al^{4+} (Table 2), in agreement with previous studies that established that nearly all the Al in omphacitic clinopyroxene tends to be in octahedral coordination. Moreover, all samples present some degree of Ca → (Fe^{2+} + Mg) substitution at the M2 site with the smaller cations occupying a M2' split position. This site has sixfold coordination similar to that observed in clinoenstatite and clinoferrosilite, which permits a more suitable coordination for Fe^{2+} and Mg. The mean atomic number of the M2' site was found to correlate with (Ca + Na) undersaturation (Rossi et al. 1987). Our data are in agreement with these previous results and confirm that the occupancy of the M2' split site depends uniquely on the bulk composition of the sample, irrespective of other effects such as the presence of vacancies.

The data refinements indicate that three of the samples (U947, Ud2290, and 90-394) have a significant number of vacancies (Table 2), which in accordance with previous studies were considered to be present only at M2 site. Attempts to refine a model with vacancies at both the M1 and at the M2 sites resulted in poor agreement factors and a crystal chemistry inconsistent with the electron microprobe analyses. McCormick (1986) reported that the presence of vacancies results in a decrease of unit-cell volume compared to samples with the same composition. To investigate the behavior of samples from this study, unit-cell volumes were plotted against Na composition and compared to

[1] Deposit item AM-07-025, Tables 3 and 4 (atomic coordinates and displacement parameters, octahedral and tetrahedral bond distances, and volumes). Deposit items are available two ways: For a paper copy contact the Business Office of the Mineralogical Society of America (see inside front cover of recent issue) for price information. For an electronic copy visit the MSA web site at http://www.minsocam.org, go to the American Mineralogist Contents, find the table of contents for the specific volume/issue wanted, and then click on the deposit link there.

Table 2. Unit-cell parameters, details of single-crystal structure refinements, and site populations of clinopyroxenes

Samples	U947	Ud2290	Ud160	Ud146	90-394	Ud94	Ud31	90-390	Ud685
a (Å)	9.5119(2)	9.5215(3)	9.5844(4)	9.6202(5)	9.6035(5)	9.6270(3)	9.6503(6)	9.6463(2)	9.6570(6)
b (Å)	8.6843(2)	8.6882(3)	8.7525(4)	8.7926(6)	8.7793(4)	8.8026(4)	8.8236(6)	8.8327(2)	8.8361(5)
c (Å)	5.2354(2)	5.2409(2)	5.2501(3)	5.2499(5)	5.2546(4)	5.2512(3)	5.2490(6)	5.2524(2)	5.2497(4)
β (°)	106.993(2)	107.069(3)	107.010(4)	107.142(5)	106.625(4)	106.939(4)	107.014(7)	106.550(2)	106.492(6)
V (Å^3)	413.58(3)	414.45(4)	421.15(5)	424.34(7)	424.51(5)	425.69(5)	427.39(10)	428.98(3)	429.53(8)
Space group	*C2/c*	*C2/c*	*C2/c*	*C2/c*	*C2/c*	*C2/c*	*C2/c*	*C2/c*	*C2/c*
No. *I* > 4σ	1247	1192	1118	1139	1170	1118	984	1301	1169
No. *I* unique	1251	1196	1133	1152	1182	1130	1115	1304	1177
R_{int}	0.01	0.02	0.01	0.02	0.02	0.01	0.02	0.01	0.01
$R_{4\sigma}$	0.023	0.024	0.023	0.040	0.033	0.026	0.036	0.032	0.023
R_{all}	0.023	0.024	0.024	0.041	0.033	0.026	0.038	0.032	0.024
GooF	1.3	1.1	1.1	1.0	1.2	1.1	1.0	1.2	1.0
No. param.	82	82	85	85	82	85	85	81	82
Site population determined by crystal-structure refinement (on 6 O atoms)									
T									
Si	1.980(1)	1.982(1)	1.990(1)	1.992(1)	1.939(1)	1.986(1)	1.996(1)	1.991(1)	1.990(1)
^{IV}Al	0.020(1)	0.018(1)	0.010(1)	0.008(1)	0.061(1)	0.014(1)	0.004(1)	0.009(1)	0.010 (1)
M1									
Ti	0.006(1)	0.005(1)	0.012(1)	0.017(1)	0.002(1)	0.015(1)	0.012(1)	0.011(1)	0.004(1)
^{VI}Al	0.652(3)	0.630(3)	0.432(3)	0.322(4)	0.438(3)	0.362(4)	0.212(3)	0.254(3)	0.250(1)
Fe^{2+}	0.037(2)	0.046(2)	0.066(2)	0.044(4)	0.042(3)	0.038(3)	0.048(4)	0.168(3)	0.064(2)
Fe^{3+}	0.008(1)	0.019(2)	0.038(1)	0.036(3)	0.008(1)	0.047(3)	0.062(4)	0.026(3)	0.010(1)
Mg	0.296(2)	0.300(2)	0.450(2)	0.579(3)	0.506(3)	0.536(3)	0.664(3)	0.540(3)	0.670(2)
Cr	0.001(1)	–	0.002(1)	0.002(1)	0.004(1)	0.002(1)	0.002(1)	0.001(1)	0.002(1)
M2									
Ca	0.374(4)	0.367(5)	0.422(4)	0.441(6)	0.625(5)	0.460(6)	0.462(7)	0.634(6)	0.694(4)
Na	0.542(3)	0.571(3)	0.482(3)	0.379(3)	0.329(3)	0.426(4)	0.294(4)	0.296(3)	0.249(3)
Mn	–	–	0.001(1)	–	–	0.002(1)	0.003(1)	0.002(1)	0.001(1)
K	0.009(1)	0.001(1)	0.003(1)	0.006(1)	0.002(1)	0.002(1)	0.003(1)	–	0.012(4)
M2'									
Fe^{2+}	0.011(2)	0.009(2)	0.048(3)	0.101(4)	–	0.085(3)	0.126(5)	0.044(3)	0.016(3)
Mg	0.013(3)	0.018(3)	0.044(3)	0.073(2)	0.013(4)	0.025(4)	0.112(5)	0.024(3)	0.028(3)
vacancies	0.051	0.034	–	–	0.031	–	–	–	–
Total	3.949	3.966	4.000	4.000	3.969	4.000	4.000	4.000	4.000

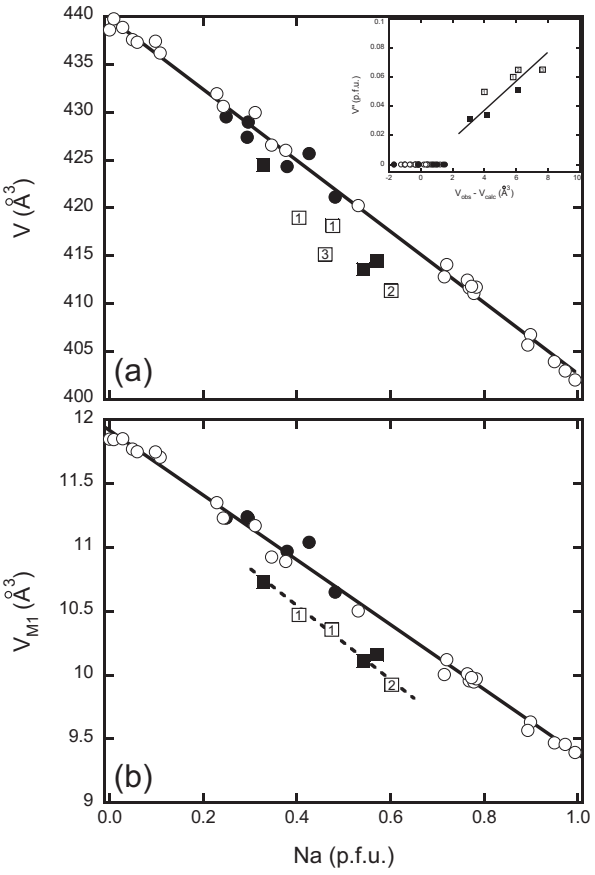

other *C*2/*c* clinopyroxenes from the literature (Fig. 1a). All of the stoichiometric pyroxenes (filled and open circles) plot close to the diopside-jadeite trend, while all vacancy-bearing samples (filled and open squares) plot significantly below this line. Such a deviation cannot be ascribed to the presence of $(Fe^{2+} + Mg)_{M2}$ (which is reported by Oberti and Caporuscio 1991 to also result in a decrease of unit-cell volume), because in the present samples the largest values of $(Fe^{2+} + Mg)_{M2}$ were obtained for the stoichiometric pyroxenes (Table 2). To investigate the deviation from the diopside-jadeite trend in greater detail, we performed a linear fit of the cell volume-Na composition data of the vacancy-free clinopyroxenes [V (Å^3) = –37.12(49) X_{Na} + 439.82(28); r^2 = 0.995] and plotted the deviation of cell volume from this trend as a function of vacancy concentration for all samples (Fig. 1b). Results show that for vacancy-bearing samples the deviation is

Figure 1. (**a**) Variation of unit-cell volume as a function of Na content for 38 *C*2/*c* omphacitic clinopyroxenes. Filled circles = vacancy-free samples (this study); filled squares = vacancy-bearing samples (this study); open circles = Cameron et al. (1973), Rossi et al. (1983), and Boffa Ballaran et al. (1998); open squares = [1] Oberti and Caporuscio (1991), [2] McCormick (1986), and [3] Smyth (1980). The solid line is a least-squares fit to the data for the vacancy-free samples. Inset: Deviation of the unit-cell volume of omphacitic clinopyroxenes from the trend defined by the stoichiometric samples (solid line in Fig. 1a) as a function of vacancy concentration. (**b**) Variation of the M1 polyhedral volume of *C*2/*c* omphacitic clinopyroxenes as a function of Na content. The solid and dotted lines are guides for the eye. The reduction of M1 site volume for vacancy-bearing samples is attributed to the substitution of Al^{3+} for Mg^{2+} to maintain charge balance (Oberti and Caporuscio 1991).

positively correlated with the concentration of vacancies. Based on our results, omphacitic clinopyroxenes with a cell volume reduction of 3 Å^3 or greater from the diopside-jadeite trend likely contain vacancies.

The positive correlation reported between cation vacancies and OH^- substitution in clinopyroxene (Smyth et al. 1991; Katayama and Nakashima 2003) implies that sample U947 should have a concentration of at least 1500 ppm (wt) H_2O, yet we measured only 89 ppm (Table 1). The possibility that hydrogen could be lost from nominally anhydrous minerals during ascent has been raised by several authors. The most likely dehydrogenation mechanism is $Fe^{2+} + OH^- \rightarrow Fe^{3+} + O^{2-} + ½\ H_2$ (e.g., Ingrin and Skogby 2000), but the maximum amount that could have been lost from sample U947 based on its Fe^{3+} concentration (Table 1) is only 380 ppm (wt) H_2O, which would suggest that vacancies were stabilized by a mechanism other than OH^- incorporation. Experiments have documented the stabilization of non-stoichiometric clinopyroxene under nominally anhydrous conditions at both high pressure (Wood and Henderson 1978; Gasparik 1986) and ambient pressure (Okui et al. 1998), where charge balance is achieved primarily through substitution of Al^{3+} for Mg^{2+} on the M1 site and causes a contraction of the M1 site volume compared to stoichiometric clinopyroxenes with the same composition (Oberti and Caporuscio 1991). Our data show a similar trend (Fig. 1).

The mechanisms suggested for OH^- incorporation in clinopyroxene (e.g., Smyth et al. 1991; Bromiley and Keppler 2004) are similar to those invoked for vacancy stabilization under anhydrous conditions (Wood and Henderson 1978; Okui et al. 1998); hence the effect of pressure on water solubility and vacancy incorporation should be similar for a given composition. The presence of vacancies in three of the samples from this study probably implies low f_{H_2O} during eclogite re-equilibration, consistent with observations that garnets from diamond-bearing eclogite xenoliths are also relatively dry (Snyder et al. 1995; Matsyuk et al. 1998). Alternatively, Withers et al. (1998) noted a decrease in water solubility in pyrope above 5 GPa that was attributed to a lower partial molar volume of water in the fluid compared to garnet, and a similar decrease of water solubility was observed in jadeite above 5 GPa (Bromiley and Keppler 2004). To date, the solubility of water in omphacitic clinopyroxene within the diamond stability field has not been experimentally determined, but could provide more robust constraints on f_{H_2O} during formation of mantle-derived eclogite, and hence insight into conditions during diamond formation.

Acknowledgments

This study is part of a larger project originally conceived by H. O'Neill, and was enhanced by the contributions of N. Ross to an earlier phase of the project. We thank J. Papike and G. D. Bromiley for reviewing and improving the manuscript. The work was supported by the Alexander von Humboldt Foundation through a fellowship award to F. Nestola and was improved through discussions with M.C. Domeneghetti and F. Camara. We are grateful to R. Rudnick and Z. Spetsius for supplying the samples, R. Rudowski for skilled hand picking of the mineral separates, and H. Keppler for the FTIR measurements. We thank H. Schulze for sample preparation and D. Krausse and A. Potzel for collecting the electron microprobe data.

References cited

Angel, R.J. (2003) Automated profile analysis for single-crystal diffraction data. Journal of Applied Crystallography, 36, 295–300.

——— (2004) Absorption corrections for diamond-anvil pressure cells implemented in the software package Absorb6.0. Journal of Applied Crystallography, 37, 486–492.

Bell, D., Ihinger, P., and Rossman, G. (1995) Quantitative analysis of trace OH in garnet and pyroxenes. American Mineralogist, 80, 465–474.

Boffa Ballaran, T., Carpenter, M.A., Domeneghetti, M.C., and Tazzoli, V. (1998) Structural mechanisms of solid solution and cation ordering in augite-jadeite pyroxenes: I. A macroscopic perspective. American Mineralogist, 83, 419–433.

Bromiley, G.D. and Keppler, H. (2004) An experimental investigation of hydroxyl solubility in jadeite and Na-rich clinopyroxenes. Contributions to Mineralogy and Petrology, 147, 189–200.

Cameron, M., Sueno, S., Prewitt, C.T., and Papike, J.J. (1973) High-temperature crystal chemistry of acmite, diopside, hedenbergite, jadeite, spodumene, and ureyite. American Mineralogist, 58, 594–618.

Carpenter, M.A. (1981) Time-temperature-transformation (TTT) analysis of cation disordering in omphacites. Contribution to Mineralogy and Petrology, 78, 433–440.

Domeneghetti, M.C., Zema, M., and Tazzoli, V. (2005) Kinetics of Fe^{2+}-Mg order-disorder in $P2_1/c$ pigeonite. American Mineralogist, 90, 1816–1823.

Ellis, D.J. and Green, D.H. (1979) An experimental study of the effect of Ca upon garnet-clinopyroxene Fe-Mg exchange. Contributions to Mineralogy and Petrology, 71, 13–22.

Gasparik, T. (1986) Experimental-study of subsolidus phase-relations and mixing properties of clinopyroxene in the silica-saturated system CaO-MgO-Al_2O_3-SiO_2. American Mineralogist, 71, 686–693.

Ingrin, J. and Skogby, H. (2000) Hydrogen in nominally anhydrous upper-mantle minerals: Concentration levels and implications. European Journal of Mineralogy, 12, 543–570.

Katayama, I. and Nakashima, S. (2003) Hydroxyl in clinopyroxene from the deep subducted crust: Evidence for H_2O transport into the mantle. American Mineralogist, 88, 229–234.

Koch-Müller, M., Matsyuk, S.S., and Wirth, R. (2004) Hydroxyl in omphacites and omphacitic clinopyroxenes of upper mantle to lower crustal origin beneath the Siberian platform. American Mineralogist, 89, 921–931.

Matsyuk, S.S., Langer, K., and Hösch, A. (1998) Hydroxyl defects in garnets from mantle xenoliths in kimberlites of the Siberian platform. Contributions to Mineralogy and Petrology, 132, 163–179.

McCormick, T.C. (1986) Crystal-chemical aspects of nonstoichiometric pyroxenes. American Mineralogist, 71, 1434–1440.

Oberti, R. and Caporuscio, F. (1991) Crystal chemistry of clinopyroxenes from mantle eclogites: a study of the key role of the M2 site population by means of crystal-structure refinement. American Mineralogist, 76, 1141–1152.

Okui, M., Sawada, H., and Marumo, F. (1998) Strcture refinement of a nonstoichiometric pyroxene synthesized under ambient pressure. Physics and Chemistry of Minerals, 25, 318–322.

Rossi, G., Smith, D.C., Ungaretti, L., and Domeneghetti, M.C. (1983) Crystal-chemistry and cation ordering in the system diopside-jadeite: a detailed study by crystal-structure refinement. Contribution to Mineralogy and Petrology, 83, 247–268.

Rossi, G., Oberti, R., Dal Negro, A., Molin, G.M., and Mellini, M. (1987) Residual electron density at the M2 site in $C2/c$ clinopyroxenes: relationships with bulk chemistry and sub-solidus evolution. Physics and Chemistry of Minerals, 14, 514–520.

Sheldrick, G.M. (1997) Programs for Crystal Structure Analysis (Release 97-2). Institüt für Anorganische Chemie der Universität, Göttingen, Germany.

Skogby, H. (2006) Water in natural mantle minerals I: Pyroxenes. In H. Keppler and J.R. Smyth, Eds., Water in Nominally Anhydrous Minerals, 62, p. 155–167. Reviews in Mineralogy and Geochemistry, Mineralogical Society of America, Chantilly, Virginia.

Smyth, J.R. (1980) Cation vacancies and crystal chemistry of breakdown reactions in kimberlitic omphacites. American Mineralogist, 65, 1185–1191.

Smyth, J.R., Bell, D.R., and Rossman, G.R. (1991) Incorporation of hydroxyl in upper-mantle clinopyroxenes. Nature, 351, 732–735.

Snyder, G.A., Taylor, L.A., Jerde, E.A., Clayton, R.N., Mayeda, T.K., Deines, P., Rossman, G.R., and Sobolev, N.V. (1995) Archean mantle heterogeneity and the origin of diamondiferous eclogites, Siberia: Evidence from stable isotopes and hydroxyl in garnet. American Mineralogist, 80, 799–809.

Stimpfl, M. (2005) The Mn,Mg-intracrystalline exchange reaction in donpeacorite ($Mn_{0.54}Ca_{0.03}Mg_{1.43}Si_2O_6$) and its relations to the fractionation behavior of Mn in Fe,Mg-orthopyroxene. American Mineralogist, 90, 155–161.

Wilson, A.J.C. (1995) International Tables for Crystallography, Volume C. Kluwer Academic Publishers, Dordrecht.

Withers, A.C., Wood, B.J., and Carroll, M.R. (1998) The OH content of pyrope at high pressure. Chemical Geology, 147, 161–171.

Wood, B.J. and Henderson, C.M.B. (1978) Compositions and unit-cell parameters of synthetic non-stoichiometric tschermakitic clinopyroxenes. American Mineralogist, 63, 66–72.

Manuscript received March 28, 2007
Manuscript accepted April 12, 2007
Manuscript handled by Bryan Chakoumakos